Carbon-nitrogen interactions in idealized simulations with JSBACH (version 3.10)

Daniel S. Goll[1,2], Alexander J. Winkler[3,4], Thomas Raddatz[3], Ning Dong[5,6], Ian Colin Prentice[5,7], Philippe Ciais[1], and Victor Brovkin[3]

[1]Le Laboratoire des Sciences du Climat et de l'Environnement, IPSL-LSCE CEA/CNRS/UVSQ Saclay, Gif sur Yvette, France.
[2]also guest scientist at Max Planck Institute for Meteorology, Hamburg, Germany
[3]Max Planck Institute for Meteorology, Hamburg, Germany
[4]International Max Planck Research School on Earth System Modelling, Hamburg, Germany
[5]Department of Biological Sciences, Macquarie University, North Ryde, NSW 2109, Australia
[6]Faculty of Agriculture and Environment, Department of Environmental Sciences, University of Sydney, NSW 2006, Australia
[7]AXA Chair in Biosphere and Climate Impacts, Department of Life Sciences, Imperial College London, Silwood Park Campus, Buckhurst Road, Ascot SL5 7PY, UK

Correspondence to: Daniel S. Goll (daniel.goll@lsce.ipsl.fr)

Abstract. Recent advances in the representation of soil carbon decomposition (Goll et al., 2015) and carbon-nitrogen interactions (Parida, 2011; Goll et al., 2012) implemented previously into separate versions of the land surface scheme JSBACH are here combined in a single version which is set to be used in the upcoming 6th phase of coupled model intercomparison project (CMIP6) (Eyring et al., 2016).

Here we demonstrate that the new version of JSBACH is able to reproduce the spatial variability in the reactive nitrogen loss pathways as derived from a compilation of $\delta^{15}N$ data (r=.63, RMSE=.26, Taylor score=.81). The inclusion of carbon-nitrogen interactions leads to a moderate reduction (-10%) of the carbon-concentration feedback (β_L) and has a negligible effect on the sensitivity of the land carbon cycle to warming (γ_L) compared to the same version of the model without carbon-nitrogen interactions in idealized simulations (1% increase in atmospheric carbon dioxide per yr). In line with evidence from elevated carbon dioxide manipulation experiments (Shi et al., 2015; Liang et al., 2016), pronounced nitrogen scarcity is alleviated by (1) the accumulation of nitrogen due to enhanced nitrogen inputs by biological nitrogen fixation and reduced losses by leaching and volatilization as well as the (2) enhanced turnover of organic nitrogen.

The strengths of the land carbon feedbacks of the recent version of JSBACH, with $\beta_L = 0.61$ Pg ppm^{-1} and $\gamma_L = -27.5$ Pg $°C^{-1}$, are 34% and 53% less than the averages of CMIP5 models (Arora et al., 2013), although the CMIP5 version of JSBACH simulated β_L and γ_L which are 59% and 42% higher than multi-model average. These changes are primarily due to the new decomposition model, stressing the importance of getting the basics right (here: the decomposition of soil carbon) before increasing the complexity of the model (here: carbon-nitrogen interactions).

1 Introduction

The version of the Max-Planck-Institute Earth System Model (MPI-ESM) used in the 5th phase of the coupled model intercomparison project (CMIP5) experienced pronounced biases in simulated soil carbon (Todd-Brown et al., 2013), soil hydrology (Hagemann and Stacke, 2014), and the lack of carbon-soil nutrient interactions (Zaehle et al., 2014; Wieder et al., 2015), ham-
5   pering the reliability of the simulated response of land system to increasing carbon dioxide (CO_2), climate and land use and land cover changes. Recent model developments addressed these issues (Goll et al., 2012, 2015; Hagemann and Stacke, 2014) in separate versions of the land surface scheme of the MPI-ESM, JSBACH, but have not been yet combined in a single model version.

The projected carbon balance in JSBACH was substantially affected by recent model developments: The implementation of
10   carbon-, nitrogen- and phosphorus interactions reduced accumulated land carbon uptake by 25% between 1860–2100 under a business as usual scenario (Goll et al., 2012), while the implementation of a new decomposition model (YASSO) reduced the accumulated land carbon uptake by about 60% in the same period (Goll et al., 2015). The exchange of the former CENTURY type soil decomposition model (Parton et al., 1993) by the YASSO decomposition model (Tuomi et al., 2008, 2009, 2011) improved the present-day state of the carbon cycle compared to observations as well as the response of decomposition to soil
15   warming, and substantially reduced the uncertainties of land use change emissions for a given land use change scenario (Goll et al., 2015). The strong impact on the carbon balance of each of both developments underline the importance of combining them in a single version.

The capacity of land ecosystems to increase their nitrogen storage as well as to enhance recycling nitrogen in organic matter are major constraints on their ability to increase carbon storage under elevated CO_2 concentrations (Hungate et al., 2003; Liang
20   et al., 2016). The respective response patterns of nitrogen processes governing the balance and turnover of organic nitrogen are crucial (Niu et al., 2016) to assess the likelihood of the occurrence of nitrogen limitation (Luo et al., 2004). Recent advances in the interpretation of soil $\delta^{15}N$ global data sets provide a promising tool (Houlton et al., 2015) by allowing a more detailed evaluation of the nitrogen loss pathways in land carbon-nitrogen models than previously done (e.g. Parida (2011); Goll et al. (2012)).

25   Since future scenarios of CO_2 concentrations differ among CMIP phases, an idealized setup of an annual increase in CO_2 concentration by 1% is used to foster the analysis of the carbon cycle feedbacks among models, and to compare emerging properties of different model versions in various CMIPs (Eyring et al., 2016). We adopt this approach taking advantage of existing simulations of climatic changes in this idealized setup of the CMIP5 intercomparison (Arora et al., 2013) to drive the land surface model JSBACH uncoupled from the atmosphere and ocean components of the earth system model.

30   This article documents the modifications to the soil carbon decomposition (Goll et al., 2015) and nitrogen cycle (Parida, 2011; Goll et al., 2012) submodels and the combination of both developments in a recent version of JSBACH including an advanced soil hydrological scheme (Hagemann and Stacke, 2014), scheduled to be used in CMIP6. We further analyzed the state of the nitrogen cycle and the carbon cycle feedbacks to increasing CO_2 concentrations and climate change. The analysis

aims at facilitating the interpretation of the models dynamics in the upcoming round of CMIP experiments (Eyring et al., 2016), and allows a straightforward comparison to the result from the previous round of CMIP (Taylor et al., 2012).

2 Methods

2.1 Model description

5   The implementation of the nitrogen cycle and the soil carbon and litter decomposition model YASSO is described in detail in Parida (2011); Goll et al. (2012) and Goll et al. (2015), respectively. In the following, a brief summary of the major concepts is given and afterwards the modification to the original developments needed to combine them are documented in detail. The notation applied here follows Goll et al. (2012, 2015).

  The YASSO decomposition model is based on a compilation of litter decomposition and soil carbon data (Tuomi et al., 2008, 10 2009, 2011). The model separates decomposing organic matter into four solubility classes (acid-soluble (C_A), water-soluble (C_W), ethanol-soluble (C_E), nonsoluble (C_N)) (Eq. 1) and an additional pool (C_H) representing humic, slowly-decomposing substances. In JSBACH the organic matter is further separated into two litter size classes, which correspond to lignified (stems and branches) and non-lignified (leaf and fine roots) litter (Goll et al., 2015).

  The interactions between nitrogen availability and plant productivity as well as decomposition are based on the concept of 15 CO_2-induced nutrient limitation (CNL) (Goll et al., 2012). In this framework, we distinguish between CNL and the background nutrient limitation. The latter is assumed to be indirectly considered in the original parametrization of carbon cycle processes as they are based on measurements in present day ecosystems and therefore reflect present day nutrient conditions. CNL is an additional nutrient limitation caused by the increase in atmospheric CO_2 and is computed dynamically according to nutrient supply and demand. In case microbial and vegetation nitrogen demand cannot be met by the supply, all carbon fluxes of which 20 the donor compartment has a higher C:N ratio than the receiving pool (i. e. the fluxes of carbon from the solubility classes pools to the humus pool) are down-regulated. The concept of CNL allows to introduce carbon-nitrogen interactions to YASSO, as the needed conditions are met, e.g. the parametrization of YASSO indirectly reflects present day nutrient effects on decomposition as it is based on leaf litter experiments.

  Following Goll et al. (2012), CNL affects the decomposition of all pools except the slowly-decomposing nutrient-rich pool, 25 which is represented by the "humus" pool in YASSO (Eqs. 2–4). The litter decomposition data on which YASSO is based is not suited to link the fate of nitrogen in litter to the respective solubility pools. Therefore, we assume one single nitrogen pool representing all nitrogen linked to the four carbon solubility pools (Eq. 6). This can be refined in the future if appropriate data becomes available.

  The nitrogen cycling is primarily driven by the nitrogen demand of the carbon cycle by the use of constant N-to-C ratios 30 of organic pools (Eqs. 5–6), with the exceptions of the non-lignified litter pool (Eq. 7) (Parida, 2011). Further exceptions are the processes linking the terrestrial carbon cycle with the atmosphere (biological nitrogen fixation and denitrification) and the aquatic systems (leaching) which are computed either as substrate-limited (Eqs. 14–15) or, for the case of biological nitrogen fixation (Eq. 13), as driven due to the ample supply of N_2 in the atmosphere (Parida, 2011). The nitrogen cycle and its

interactions with the carbon cycle are not modified. The only exception is that the turnover times of the nitrogen litter and soil organic matter pools are derived from the YASSO decomposition model (Eq. 9) instead of the former decomposition model. All parameters and variables are given in Table 1&2

2.1.1 Nitrogen effect on decomposition

5 Matrix $\mathbf{C}$ describes the soil carbon pools (A, W, E, N, H) of the two litter size classes (i) in JSBACH:

$$
\mathbf{C_i} = \begin{pmatrix} C_{A,i} \\ C_{W,i} \\ C_{E,i} \\ C_{N,i} \end{pmatrix}
\tag{1}
$$

The dynamics of the soil carbon pools are described as

$$
\frac{d\mathbf{C_i}}{dt} = \mathbf{A_p}\mathbf{k_i}(\mathbf{F})\mathbf{C_i} + \mathbf{I_i}
\tag{2}
$$

where $\mathbf{A_p}$ is the mass flow matrix; $\mathbf{k}(\mathbf{F})$ is a diagonal matrix of the decomposition rates $\mathbf{k_i}(\mathbf{F}) = diag(k_{A,i}, k_{W,i}, k_{E,i}, k_{N,i})(\mathbf{F})$
10 as a function of climatic conditions ($\mathbf{F}$); and matrix $\mathbf{I_i}$ is the carbon input of type i to the soil. A detail description of decomposition can be found in the supplementary information of Goll et al. (2015), here we only focus on the modification of the original implementation.

The climate dependence of the decomposition rate factor $k_{j,i}$ of the carbon pools was originally implemented by Goll et al. (2015) based on Tuomi et al. (2008) as:

15 $$k_{j,i}(\mathbf{F}) = \alpha_{j,i}exp(\beta_1 T + \beta_2 T^2)(1 - exp(\gamma P)),
\tag{3}$$

where T is air temperature and P is precipitation, β_1, β_2, γ are parameters, and $\alpha_{j,i}$ are decomposition rates at references conditions ($T = 0$ and $P \to \infty$) of pool i of litter class j. $\alpha_{j,i}$ is the product of a reference decomposition rate of solubility class j and the litter diameter of litter class i (Tuomi et al., 2011). YASSO uses precipitation instead of the more direct driver of soil moisture due the lack of adequate soil moisture observation to relate the decomposition date the model is based on (Tuomi
20 et al., 2008).

We introduced a scaling factor, namely the nitrogen limitation factor (f_{limit}^N), to account for the down-regulation of decomposition when nitrogen is in short supply

$$
k_{j,i}(\mathbf{F}) = f_{limit}^N\alpha_{j,i}exp(\beta_1 T + \beta_2 T^2)(1 - exp(\gamma P)),
\tag{4}
$$

f_{limit}^N is calculated based on a supply and demand approach (Parida, 2011; Goll et al., 2012). In a first step, potential carbon
25 fluxes are computed from which the release and immobilization of mineral nitrogen is diagnosed. In a second step, all fluxes consuming nitrogen (donor compartment has a higher C:N ratio than the receiving pool) are down-regulated in case nitrogen demand cannot be met by the nitrogen supply. In case nitrogen demand is met by the supply, the fluxes computed in the first step are taken as actual ones without any modification.

Table 1. Variables of the model.

Variable	Units	Description
P	m day^{-1}	30 days average of daily precipitation
T	$^\circ$C	30 days average of daily 2m air temperature
$C_{j,i}$	mol(C) m^{-2}	soil organic carbon of solubility class j and size class i
N_x	mol(N) m^{-2}	nitrogen in compartment x
$\overline{NPP}$	mol(C) m^{-2} day^{-1}	annual average of daily net primary productivity
$F^C_{x \triangleright y}$	mol(C) m^{-2} day^{-1}	daily flux of carbon from compartment x to compartment y
F_{extr}	mol(C) m^{-2} day^{-1}	daily flux of nitrogen in excrements
F_{extr}	mol(C) m^{-2} day^{-1}	daily flux of nitrogen lost by leaching
BNF	mol(N) m^{-2} day^{-1}	daily nitrogen inputs by biological nitrogen fixation
D_x	mol(N) m^{-2} day^{-1}	nitrogen demand of vegetation ($x = veg$) or immobilization ($x = micr$)
f^N_{limit}	–	nitrogen limitation factor
d_x	day^{-1}	decomposition rate of nitrogen in compartment x
$k_{j,i}$	day^{-1}	decomposition rate of solubility class j and size class i
k_H	day^{-1}	decomposition rate of humus pool
ϵ	day^{-1}	consumption rate by herbivores
f_{h2o}	–	daily fraction of soil water lost due to runoff and drainage
α	–	soil moisture stress on biological processes

2.1.2 Dynamics of nitrogen in litter and soil organic matter

We substituted the former carbon pools for slowly-decomposing organic matter C_s, lignified litter and fast decomposing organic matter C_{lw}, as well as non-lignified litter and fast decomposing organic matter C_{la} with the corresponding YASSO pools (Table 3) to derive the dynamics of the nitrogen pools.

5  In JSBACH, nitrogen in compartments with a fixed N-to-C ratio, namely nitrogen in lignified litter (N_{lw}) as well as nitrogen in slowly decomposing organic matter (N_s), are derived from the corresponding YASSO carbon pools ($C_{j,i}$) by:

$$N_s = r_s C_H \tag{5}$$

$$N_{lw} = r_{lw}(C_{A,w} + C_{W,w} + C_{E,w} + C_{N,w}) \tag{6}$$

where r_s is the N-to-C ratio of former slow carbon pool (C_s) now applied to the humus pool of YASSO, and r_{lw} of former
10 woody litter pool (C_{lw}) now applied to the sum of the solubility class pools for lignified litter of YASSO.

Table 2. Parameters of the model. $^{(*)}$ $\alpha_{j,i}$ is an array and values can be found in Tuomi et al. (2011).

Parameter	Value	Units	Description	Source
β_1	0.095	$^\circ\mathrm{C}^{-1}$	Temperature dependence of decomposition	Goll et al. (2015)
β_2	-1.4×10^{-3}	$^\circ\mathrm{C}^{-2}$	Temperature dependence of decomposition	Goll et al. (2015)
γ_1	-1.21	m^{-1}	Precipitation dependence of decomposition	Goll et al. (2015)
$\alpha_{j,i}$	$^{(*)}$	day^{-1}	decomposition rates at references conditions	
			($T = 0$ and $P \to \infty$) of pool i of litter class j	Tuomi et al. (2011)
α_H	4.383×10^{-6}	day^{-1}	decomposition rates at references conditions	
			($T = 0$ and $P \to \infty$) of humus pool	Tuomi et al. (2011)
r_s	10.	$\mathrm{mol(N)\,mol^{-1}(C)}$	N-to-C ratio of slowly decomposing organic matter	Goll et al. (2012)
r_{lw}	330.	$\mathrm{mol(N)\,mol^{-1}(C)}$	N-to-C ratio of lignified litter	Goll et al. (2012)
r_{la}	55.	$\mathrm{mol(N)\,mol^{-1}(C)}$	N-to-C ratio of non-lignified litter	Goll et al. (2012)
r_w	150.	$\mathrm{mol(N)\,mol^{-1}(C)}$	N-to-C ratio of lignified biomass	Goll et al. (2012)
β_3	0.7	–	fraction of nitrogen in excrement in labile form	Parida (2011)
f_{emp}	-3.0×10^{-3}	$\mathrm{day\,g^{-1}(C)}$	NPP dependence of biological nitrogen fixation	Cleveland et al. (1999)
f_{bnf}	0.7	$\mathrm{g(N)\,m^{-2}\,day^{-1}}$	scaling factor of biological nitrogen fixation	this study
f_s	0.1	–	fraction of soil mineral nitrogen in soil solution	this study
k_{denit}	2.0×10^{-3}	–	daily fraction of soil mineral nitrogen lost by denitrifcation	Parida (2011)
w_C	12.011	$\mathrm{g(C)\,mol^{-1}(C)}$	standard atomic weight of carbon	
w_N	14.007	$\mathrm{g(N)\,mol^{-1}(N)}$	standard atomic weight of nitrogen	
t	1	day	time step	

Table 3. The nitrogen pools and the corresponding carbon pools.

Nitrogen	Carbon
N_s	C_H
N_{lw}	$C_{A,w} + C_{W,w} + C_{E,w} + C_{N,w}$
N_{la}	$C_{A,g} + C_{W,g} + C_{E,g} + C_{N,g}$

The dynamics of nitrogen in non-lignified litter & fast decomposing organic matter (N_{la}) were not modified from the original nitrogen-enabled version of JSBACH (Parida, 2011) and are given by:

$$\frac{dN_{la}}{dt} = r_{la}F^C_{a\triangleright la} + (1-\beta_3)\epsilon N_a - f^N_{limit}d_{la} * N_{la} \tag{7}$$

where the first term describes the nitrogen influx from active, non-lignified plant tissue (N_a), the second term describes the

5 flux of nitrogen from herbivores excrements which is not directly available to biota, and the third term arises from the nitrogen released by biological mineralization of litter and fast-decomposing soil organic matter, where f^N_{limit} is the limitation factor. We assume that active plant material (N_a) is consumed by herbivores at a constant rate (ϵ) and immediately excreted (Parida, 2011). We separate the excrement into labile (β_3) and fast decomposing ($1-\beta_3$) nitrogen compounds, the latter enters the non-lignified litter pool (N_{la}).

10 The decomposition rate d_{la} of nitrogen in litter and fast decomposing soil organic matter equals the decomposition rate of the sum of the YASSO carbon pools $C_{A,g} + C_{W,g} + C_{E,g} + C_{N,g}$ and is given by

$$\frac{d(C_{A,g} + C_{W,g} + C_{E,g} + C_{N,g})}{dt} = d_{la}(C_{A,g} + C_{W,g} + C_{E,g} + C_{N,g}) \tag{8}$$

so that d_{la} can be derived from

$$d_{la} = \frac{C_{A,g}(t+1) + C_{W,g}(t+1) + C_{E,g}(t+1) + C_{N,g}(t+1)}{C_{A,g}(t) + C_{W,g}(t) + C_{E,g}(t) + C_{N,g}(t)} - 1 \tag{9}$$

15 As we calculate potential decomposition fluxes in a first step to derive nitrogen demand (see Goll et al. 2012) we know the state of pools for time t and $t+1$.

The dynamics of the soil mineral nitrogen (N_{smin}) were not modified and are given - as originally formulated by Parida (2011) - by:

$$\frac{dN_{smin}}{dt} = F_{extr} + d_s N_s + (r_w - r_{lw})F^C_{w\triangleright lw} - f^N_{limit}(D_{veg} + D_{micr}) \tag{10}$$

20 where F_{extr} is the net of fluxes connecting the compartments considered in the model and outside (here: biological dinitrogen (N_2) fixation, leaching, N_2 and nitrous oxide (N_2O) emissions), r_w the N-to-C ratio of lignified plant material, $F^C_{w\triangleright lw}$ the litter flux from lignified biomass, D_{micr} and D_{veg} are the nitrogen demands of vegetation and microbes, respectively. The decomposition rate of nitrogen in the slow pool (N_s), d_s, equals the decomposition rate of the corresponding YASSO carbon pool C_H, k_H. This rate according to Eq.(3) is given by:

25 $$k_H(\mathbf{F}) = \alpha_H exp(\beta_1 T + \beta_2 T^2)(1 - exp(\gamma P)), \tag{11}$$

Note that there is no nutrient effect on the decomposition of N_s and k_H is calculated exactly like described in Goll et al. (2015).

For the calculation of the microbial (soil) nutrient demand (D_{micr}) we substituted the pools C_{la} and C_s with the corresponding YASSO pools in Eq.(15) of Goll et al 2012:

$$D_{micr} = (r_s - \frac{N_{la}}{(C_{A,g} + C_{W,g} + C_{E,g} + C_{N,g})})F^C_{la\triangleright s} + (r_s - r_{lw})F^C_{lw\triangleright s} - \frac{N_{la}}{(C_{A,g} + C_{W,g} + C_{E,g} + C_{N,g})})F^C_{la\triangleright a} - r_{lw}F^C_{lw\triangleright a}$$

$$(12)$$

The fluxes $F^C_{la \triangleright s}$ and $F^C_{lw \triangleright s}$ are the net fluxes of carbon to the humus from the solubility pools (AWEN) of non-lignified and lignified litter, respectively. $F^C_{la \triangleright a}$ and $F^C_{lw \triangleright a}$ are the respective sums of respiration fluxes of the AWEN pools.

2.2 The processes governing the terrestrial nitrogen balance in JSBACH

Nitrogen enters terrestrial ecosystems by biological nitrogen fixation (BNF), as well as atmospheric deposition, while lost via leaching, erosion and denitrification.

BNF in global models is commonly represented by an empirical relationship based on a compilation of site measurements (Cleveland et al., 1999). Due to the lack of a process-based alternatives, we use this approach as described in Parida (2011) despite its shortcomings (Thomas et al., 2013; Sullivan et al., 2014; Wieder et al., 2015). In this approach BNF (BNF) is derived from the annual average of daily net primary productivity ($\overline{NPP}$) using the empirical relationship between BNF and evapotranspiration (Thornton et al., 2007):

$$BNF = (f_{bnf} * (1 - e^{(f_{emp} w_C \overline{NPP})}) \frac{w_N}{w_C} \tag{13}$$

where $f_{emp} = -0.003$ day g^{-1}(C) is an empirical relationship from Cleveland et al. (1999) , $f_{bnf} = 0.7$ g(N) m^{-2} day^{-1} is a calibrated constant to achieve a global sum of BNF of 100 Mt yr^{-1} for a simulated NPP of 65 Gt yr^{-1} based on estimates for present day (Galloway et al., 2013; Ciais et al., 2013), and w_N and w_C the standard atomic weights of nitrogen and carbon, respectively.

Following Meixner and Bales (2002); Thornton et al. (2007); Parida (2011), daily losses by leaching are derived from dissolved nitrogen in soil water and the fraction of soil water lost to rivers per day (f_{h2o}) assuming a homogeneous distribution of mineral nitrogen (N_{smin}) in the soil volume :

$$F_{leach} = f_s N_{smin} f_{h2o} \tag{14}$$

where f_s is the fraction of mineral nitrogen (N_{smin}) in soil solution.

Following Parida (2011); Goll et al. (2012), daily losses by denitrification are assumed to be at most 0.02% ($k_{denit} = 0.002$ day^{-1}) of the soil mineral (N_{smin}):

$$F_{denit} = \alpha k_{denit} N_{smin} \tag{15}$$

where α is a JSBACH internal indicator of soil moisture stress [0–1] which is dynamically computed from soil moisture and used to scale biological activity (Raddatz et al., 2007).

2.3 Calibration & parametrization of the model

The parametrization of YASSO (version 3.20) and of the nitrogen cycle in JSBACH was not changed and is described in Goll et al. (2012, 2015). The only exception is the re-calibration of losses of nitrogen by leaching to the new hydrological model

Table 4. Simulations performed with JSBACH with and without carbon-nitrogen interactions using climatic forcing from MPI-ESM simulations performed for the CMIP5 project (Taylor et al., 2012).

Acronym	C-N interactions	climatic forcing	description
C	without	1pctCO2	1% yr^{-1} increase in CO_2 (to quadrupling)
C_β	without	esmFdbkl	Carbon cycle sees piControl CO_2 concentration, but radiation sees 1% yr^{-1} rise
C_γ	without	esmFixClim1	Radiation sees piControl CO_2 concentration, but carbon cycle sees 1% yr^{-1} rise
CN	with	1pctCO2	1% yr^{-1} increase in CO_2 (to quadrupling)
CN_β	with	esmFdbkl	Carbon cycle sees piControl CO_2 concentration, but radiation sees 1% yr^{-1} rise
CN_γ	with	esmFixClim1	Radiation sees piControl CO_2 concentration, but carbon cycle sees 1% yr^{-1} rise

in JSBACH (Hagemann and Stacke, 2014). This is achieved, following Goll et al. (2012), by tuning the fraction of mineral nitrogen in soil solution (f_s) so that the assumption regarding the absence of CNL in the pre-industrial state is met. We tuned the the fraction of soil mineral nitrogen in soil solution to $f_s = 0.1$, which is lower than in an earlier version (0.2) (Parida, 2011) and in the range of others model (0.02–1.) (Esser et al., 2011; Wang et al., 2010; Warlind et al., 2014).

2.4 Simulation setup

The climatic forcing is derived from MPI-ESM simulations performed for the CMIP5 project (Table 4) (Taylor et al., 2012). We force the land surface model JSBACH with half hourly climatic data simulated by the MPI-ESM instead of running JSBACH coupled with the atmospheric and ocean components of the MPI-ESM. Therefore, our simulations, in contrast to simulations of the MPI-ESM, do not account for the feedback between land and atmosphere with respect to the water and energy cycle. However, the resulting inconsistencies between climate and land surface should not cchange the results of the present study and are anyway partly implicit to the underlying CMIP5 simulations because of the prescribed atmospheric CO_2 levels in case of biogeochemical feedbacks (Taylor et al., 2012). For the sake of simplicity, we will refer to the JSBACH simulations driven by the climate from respective ESM simulations, with the respective label of the ESM simulations.

2.4.1 Spinup

The concept of CO_2 induced nutrient limitation (CNL) assumes that nitrogen effects on the carbon cycle are marginal under pre-industrial conditions. Therefore the cycles of carbon and nitrogen can be equilibrated in a two-step procedure in which the carbon cycle is first brought into equilibrium (less than 1% change in global stocks per decade) using the climatic forcing from the pre-industrial control run (Goll et al., 2012). In a second step, we then initialize the nitrogen pools using the prescribed

C:N ratios and the equilibrated carbon stocks as well as extremely high mineral nitrogen pools. The model is run again with the climatic forcing from the pre-industrial control run to equilibrate mineral nitrogen dynamics using the same criterion as for the first step. The resulting length of the simulation is 5.5 kyr and 2.6 kyr for step one and step two, respectively. Atmospheric nitrogen depositions are neglected.

2.4.2   1% CO$_2$ increase experiment & climate feedback factors

To analyze the effect of nitrogen limitation on the response of the land carbon cycle to increasing CO$_2$ concentration and climate change, we perform simulations with JSBACH with and without activated nitrogen cycle (Table 4). The simulations are forced with the climatic conditions from a set of 140 yr long CMIP5 simulations with the MPI-ESM in which atmospheric CO$_2$ concentration increases at a rate of 1% yr^{-1} from pre-industrial values until concentration quadruples (Arora et al., 2013).

The set of MPI-ESM simulations consist of a simulation where increasing CO$_2$ affects the climate but not the terrestrial biogeochemistry (radiatively coupled), a second simulation where increasing CO$_2$ affects the terrestrial biogeochemistry but not the climate (biogeochemically coupled), and a third simulation where increasing CO$_2$ affects both, climate and biogeochemistry (fully coupled). The biogeochemically-coupled and the radiatively coupled simulations allow us to disentangle the carbon-concentration feedback β_L and carbon-climate feedback γ_L, respectively (Friedlingstein et al., 2006; Arora et al., 2013). β_L is derived from the biogeochemically coupled simulations by dividing the difference in the total land carbon between the first and the last decade by the difference in the atmospheric CO$_2$ concentration of the same periods. γ_L is derived from the radiatively coupled simulations by dividing the difference in the total land carbon between the first and the last decade by the difference in global land temperature of the same periods. The MPI-ESM simulations do not include the confounding effects of changes in land use, non-CO$_2$ greenhouse gases, aerosols, etc., and so provide a controlled experiment with which to compare carbon climate interactions in line with the approach by Arora et al. (2013). The model version also does not include dynamic vegetation model and disturbances, such as fire. Natural vegetation cover is prescribed following approach by Pongratz et al. (2008). Cropland and pasture map for 1850 is taken from harmonized landuse dataset by Hurtt et al. (2011).

2.5   Analysis

2.5.1   Pre-industrial state

We average the model data of last three decades of the spinup simulations to derive the pre-industrial state. Differences between model and observation are given by the subtraction of the observation with the simulation. The fraction of denitrification losses to total losses is computed by dividing the annual flux of denitrification by the sum of the annual fluxes of denitrification and leaching. Simulated and observation loss fractions are compared using Pearson correlation coefficients, RMSE, and Taylor scores (Taylor, 2001).

2.5.2 Nitrogen loss pathway data

The fraction of N loss in gaseous form (f_{denit}) was estimated using the principle described by e.g. Houlton and Bai (2009); Bai et al. (2012), but using a process-based statistical model for the relationship between soil δ15N data and environmental predictors fitted to publicly available data on soil δ15N (Patino et al., 2009; Cheng et al., 2009; McCarthy and Pataki, 2010; Fang et al., 2011, 2013; Hilton et al., 2013; Peri et al., 2012; Viani et al., 2011; Sommer et al., 2012; Yi and Yang, 2007).

It was assumed that soil δ^{15}N reflects the source (atmospheric) δ^{15}N modified by isotopic discrimination that occurs during leaching (slight) and gaseous losses (much larger). For simplicity, the source δ^{15}N was assumed to be zero and discrimination during leaching was neglected. Mean annual runoff (q, in [mm]) was estimated from precipitation and potential evapotranspiration following (Zhang et al., 2004), with $\omega = 3$. Following Xu-Ri et al. (2008) we assumed that leaching losses increase to a maximum dependent on soil water capacity, yielding an annual runoff factor f(q):

$$f(q) = \frac{q}{q + W_{max}} \tag{16}$$

with $W_{max} = 150mm$. Mean monthly soil temperatures (T_m, in K) were estimated for 0.25 m depth following Campbell and Norman. We assigned a generic activation energy of $E_a = 55 kJmol^{-1}K^{-1}$ (Canion et al., 2014) and summed the monthly index values

$$f_m(T_m) = exp(\frac{E_a}{R_{gas}}(\frac{1}{T_{ref}} - \frac{1}{T_m})) \tag{17}$$

over the 12 months

$$f(T) = \sum_{m=1}^{12} = f_m(T_m) \tag{18}$$

yielding the annual soil temperature factor $f(T)$, where $T_{ref} = 293K$.

The data were then fitted by non-linear least-squares regression to the relationship

$$\delta = \delta_0 + \epsilon(1 + k(\frac{f(q)}{f(T)}))^{-1} \tag{19}$$

where δ is soil δ^{15}N, δ_0 is the δ^{15}N of the N inputs, ϵ is the gaseous discrimination factor and k is a constant to be estimated. Assuming the leaching discrimination factor is 0, f_{denit} can be expressed as

$$f_{denit} = \frac{\delta - \delta_0}{\epsilon} \tag{20}$$

from the first principle (Houlton and Bai, 2009). The global values of f_{denit} were derived from the calculated values of $f(q)$ and $f_m(T_m)$ across each grid cell based on monthly grids of observed mean climate from 1961–1990 covering the global land surface at a 10 minute spatial resolution (CRU CL2.0) (New et al., 2002).

Table 5. Comparison of simulated net primary productivity as well all mineral nitrogen stocks and fluxes for pre-industrial conditions with observation based estimates for 1850 and present day.

	simulated	observation-based		
	1850	1850	present day	reference
NPP (Gt yr^{-1})	65.1	–	50–56	Ito (2011)
leaching (Mt yr^{-1})	50.0	70	13–180	Galloway et al. (2004, 2013)
denitrification (Mt yr^{-1})	49.2	–	43–290	Galloway et al. (2013)
BNF (Mt yr^{-1})	98.3	40–120	100–139	Galloway et al. (2004); Vitousek et al. (2013)
Mineral nitrogen (Gt)	1.3	–	–	
Total nitrogen (Gt)	63.6	–	60–75	Galloway et al. (2013)

3   Results & discussion

3.1   Model evaluation: pre-industrial state

The model simulates mineral nitrogen stocks and fluxes well within the wide range of estimates (Table 5). The simulated losses by leaching and denitrification are rather at the lower end of estimates, while the calibrated inputs by biological nitrogen
5   fixation are at the higher end of estimates.

The organic nitrogen stocks and fluxes are given by the prescribed C:N stoichiometry and the state variables of the carbon cycle and thus are not affected by the changes we introduced here. Thus, we refer to the evaluation of the carbon cycle in JSBACH elsewhere (Anav et al., 2013; Goll et al., 2015), as the concept of CO_2 induced nutrient limitation prevents an effect of nitrogen on the carbon cycle under pre-industrial CO_2 concentrations.

10   The large uncertainty in estimates of global fluxes and stocks of nitrogen hampers a detailed analysis of the simulated nitrogen cycle (Zaehle, 2013). However, recent advances in the use of $\delta^{15}N$ data (Houlton et al., 2015) allow the evaluation of the respective importance of nitrogen loss pathways in space. Due to the different environmental controls of the loss pathways, which are on first order represented in the model, we can test the models assumptions by comparing the simulated fraction of denitrification losses to total nitrogen losses (f_{denit}) to f_{denit} reconstructed from $\delta^{15}N$ data.

15   We estimate from collected $\delta^{15}N$ data the highest values of fractional gaseous loss in arid regions, where leaching losses are minimal in these regions. Gaseous N loss is also predicted to be the dominant pathway over much of the tropics, with lower values towards high latitudes. The pattern is generally consistent with earlier estimates of f_{denit} from Houlton et al. (2015).

In comparison with the reconstructed fractional gaseous loss, we find that the model is in rather good agreement (Pearson R=0.63, RMSE=0.26, Taylor score=0.81). However, some regions substantially differ between model and observation (Fig-
20   ure 1) which can be attributed to the use of the MPI-ESM climate which in some regions deviates significantly from the observed climate: The biases in denitrification losses resemble biases in surface temperature and precipitation in the climatic forcing from MPI-ESM (Hagemann et al., 2013). The strong underestimation of denitrification losses at the West-coast of
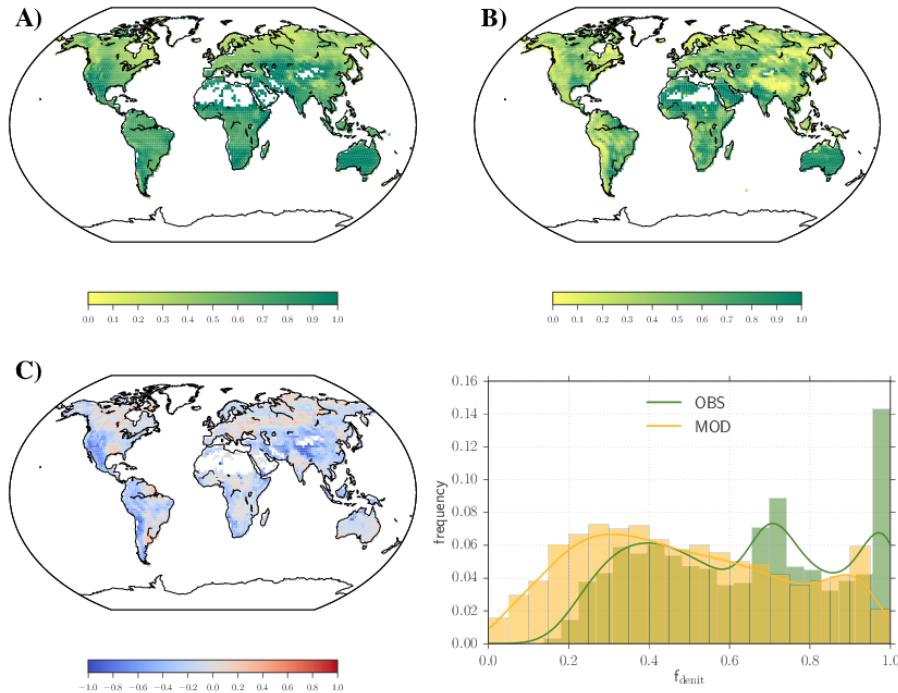
Figure 1. Comparison of simulated and reconstructed fractions of nitrogen lost by denitrification relative to total losses (f_{denit}). Shown are loss fractions reconstructed from observational data on $\delta^{15}N$ (a), as simulated (b), the difference between simulated and reconstructed f_{denit} (c), as well as the frequency distribution of simulated (yellow) and reconstructed (green) f_{denit} (d).

Table 6. Simulated response ratios of gross and net primary productivity to elevated CO_2 in comparison with observation based estimates.

Response ratio	simulated	observed	reference
GPP_{396}/GPP_{295}	1.23±0.03	1.25	Ehlers et al. (2015)
NPP_{550}/NPP_{370}	1.16±0.03	1.23±0.02	Norby et al. (2005)

North and South America, Central Asia, and the Southwest coast of Africa can be attributed to the strong overestimation of precipitation in the climatic forcing compared to observations (Weedon et al., 2011; Hagemann et al., 2013). The pronounced positive bias in boreal winter temperatures of 0.5–5.5 K between 40–80°N in Eurasia as well as East part of North America resembles regions with a strong overestimation of denitrification losses. The frequency distribution of simulated and observed f_{denit} indicates that the occurence of regions of where denitrifcation dominates are underestimated while regions where leaching dominates are overestimated in the model.
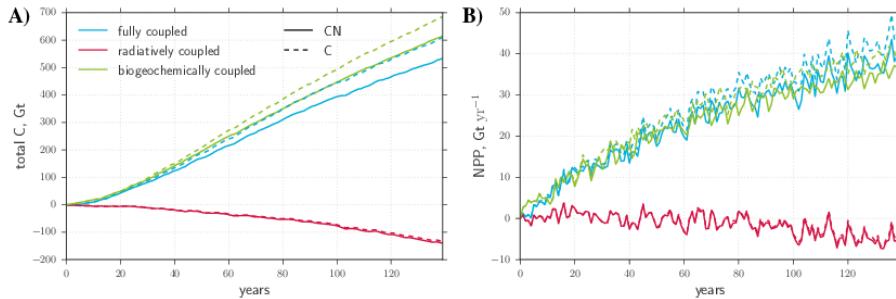
Figure 2. Changes in global net primary productivity (a) and total land carbon (b) in the set of 1% CO_2 increase simulations with (solid line) and without (dashed line) carbon-nitrogen interactions.

3.2   Changes in the land carbon cycle in the 1% CO_2 increase simulations

JSBACH simulates a strong increase in net plant productivity (NPP) due to increasing CO_2 from pre-industrial level to 4 × pre-industrial level (Figure 2). The simulated increase in NPP of 16.0% for a rise in atmospheric CO_2 from 370 ppm to 550 ppm is somewhat lower than the estimated increase of 25% from 4 free air carbon dioxide enrichment (FACE) experiments 5   (Norby et al., 2005) (Table 6). A lower increase than in the FACE experiment can be expected as the long-term effect of elevated CO_2 is likely to be less than the one derived from short duration FACE experiments (Norby et al., 2010) on early successional forests (Norby et al., 2015). The simulated increase in GPP of 23.1% for an increase in atmospheric CO_2 concentration from the level of the year 1900 to 2013 is close to the 25% increase for the same increase in CO_2 estimated from intramolecular isotope distributions (isotopomers), a methodology for detecting shifts in plant carbon metabolism over long times (Ehlers 10   et al., 2015).

The increase in NPP translates to an increase in carbon storage of approximately 600 Gt by end of the biogeochemically-coupled simulation (Figure 2). Climate change, in particular increasing temperature, overall has a slightly negative effect on global NPP: the carbon losses by autotrophic respiration in low latitudes outweigh the increases in NPP in temperature limited ecosystems. Globally, warming stimulates the decomposition of soil organic matter (not shown) which leads to a smaller 15   increase in carbon storage in the fully-coupled simulation compared to the biogeochemically-coupled simulation, and even a reduction in carbon storage in the radiatively-coupled simulations. The effect of CO_2 and climate change on land carbon storage is much less pronounced in the recent version of JSBACH than in the CMIP5 version and the responses of the new version lie well within the range of CMIP5 models (Arora et al., 2013). The more moderate response can mainly be attributed to the recent improvement in respect to the carbon cycle and are discussed in detail later.

20   3.3   Changes in the land nitrogen cycle in the 1% CO_2 increase simulations

Increasing atmospheric CO_2 concentration leads to the accumulation of nitrogen in the terrestrial system (Figure 3a), due to elevated inputs by biological nitrogen fixation (BNF) (Figure 3c) in combination with reduced losses by leaching and denitrification (Figure 3d). The increasing primary productivity and the subsequent incorporation of soil mineral nitrogen are
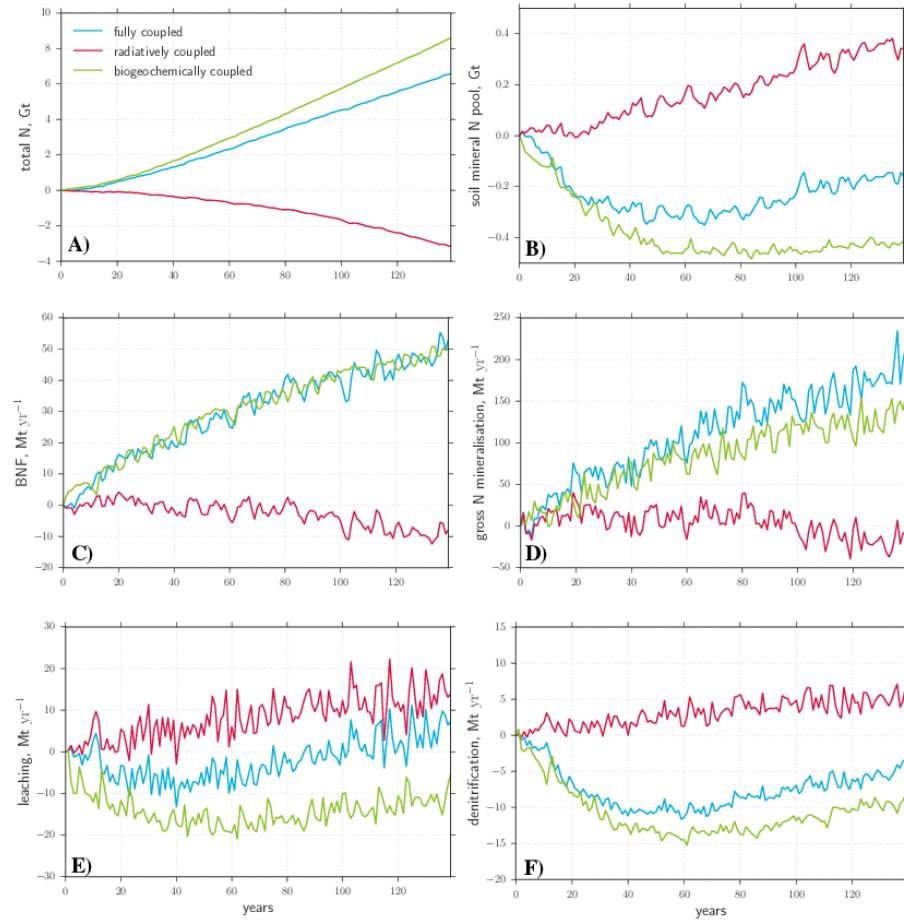
Figure 3. Changes in the nitrogen cycling in the set of 1% CO_2 increase simulations with carbon-nitrogen interactions: (a) total nitrogen, (b) mineral N, (c) biological nitrogen fixation, (d) net mineralisation, (e) leaching, and (f) denitrification.
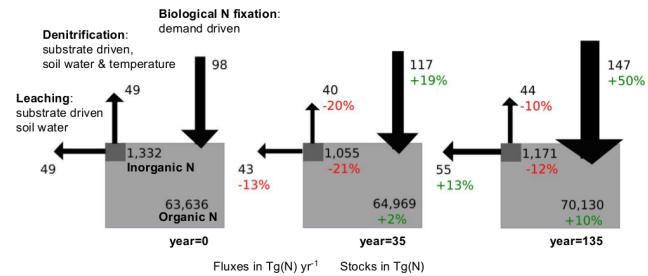
Figure 4. The terrestrial nitrogen balance during the fully "coupled" simulation. Shown are the average fluxes and stocks for 10 yr time period for initial conditions (year=0; 284 ppm), fourth decade (year=35; 400ppm) and the last decade (year=135; 4 × 284 ppm).

the main drivers behind the accumulation. Increasing NPP (Figure 2) directly stimulates the demand-driven process of BNF and therefore BNF rates increase nearly as strong as NPP (50% compared to 59% by end of the simulations). The decline in soil mineral nitrogen (Figure 3b) due to the incorporation of nitrogen in accumulating biomass leads to reduced losses by leaching and denitrification.

5   An increase in the nitrogen stock by 8.5% was found in a 15-yr ecosystem scale CO_2 enrichment experiment (Shi et al., 2015), which is more pronounced than the simulated increase in the nitrogen stock of 3.2% for a comparable increase in CO_2 (year 29–69; 369–551ppm). A strong stimulation of BNF by 44%, with a strong decline in leaching by 42% and no significant changes in denitrification, mineralisation and soil organic nitrogen were found in a compilation of CO_2 enrichment experiments (Liang et al., 2016). However the representativeness of these findings was questioned recently (Rütting, 2016). In

10   addition to that, CO_2 was increased abruptly in CO_2 enrichment experiments while it increased gradually in our simulations. As the different nitrogen processes have different response patterns, they are likely to react differently to an abrupt than to a gradual increase in CO_2. Although the relative contributions of reduced losses and increased inputs to an accumulation remain somewhat elusive due to methodological biases (Rütting, 2016) and limited data, an accumulation of nitrogen under elevated CO_2 is a plausible scenario.

15   We find that the processes governing the nitrogen balance operate on different time scales (Figure 4). The mineral nitrogen stocks decline from 1.33 Gt to 1.06 Gt during the first 35 yrs and thereby reduce the substrate driven nitrogen losses (Figure 4) from 98 Mt yr^{-1} to 83 Mt yr^{-1}. However, losses by leaching start to increase afterwards and are higher by the end of the simulation than at the start. While the reduction in losses and gains in inputs contribute to equally parts to the accumulation in the first decades of the simulation, the stimulated BNF dominates the accumulation in later (Figure 4). This highlights the

20   importance of long term manipulation experiments for improving our understanding about the long term effects of increasing CO_2 on the terrestrial biosphere.

    We find that the effect of increasing CO_2 and climate change on the nitrogen balance differ. Elevated CO_2 alone leads to a shift from inorganic nitrogen to organic nitrogen (Figure 3a&b), whereas climate change is dampening this shift as warming stimulates the decomposition of organic nitrogen (Figure 3d) and thereby slow down the progressive immobilization of mineral

25   nitrogen into biomass and soil organic matter. Climate change alone leads to a loss of nitrogen from the system (Figure3a): The enhanced net mineralisation of organic nitrogen due to warming leads to increased losses of nitrogen via leaching and denitrification. We further found that changes in the water cycle due to climate change are increasing losses by leaching, while denitrification follows primarily the changes in substrate availability despite the influence of soil moisture in Eq. 15 (Figure 4). Overall, we find that total nitrogen losses are intensified relative to the substrate availability at the end compared to the start of

30   the simulations (Figure 4).

    The overall behavior of the nitrogen cyle is in line with the substrate-based mechanisms proposed based on recent compilation of ecosystem nitrogen addition experiments (Niu et al., 2016), in which the mineral nitrogen exerts a major control on the mineral nitrogen consuming processes. However, the respective observed response patterns of ecosystem nitrogen processes remain to a large degree unknown and are represented in a strongly simplified way in JSBACH . In general, we find that the
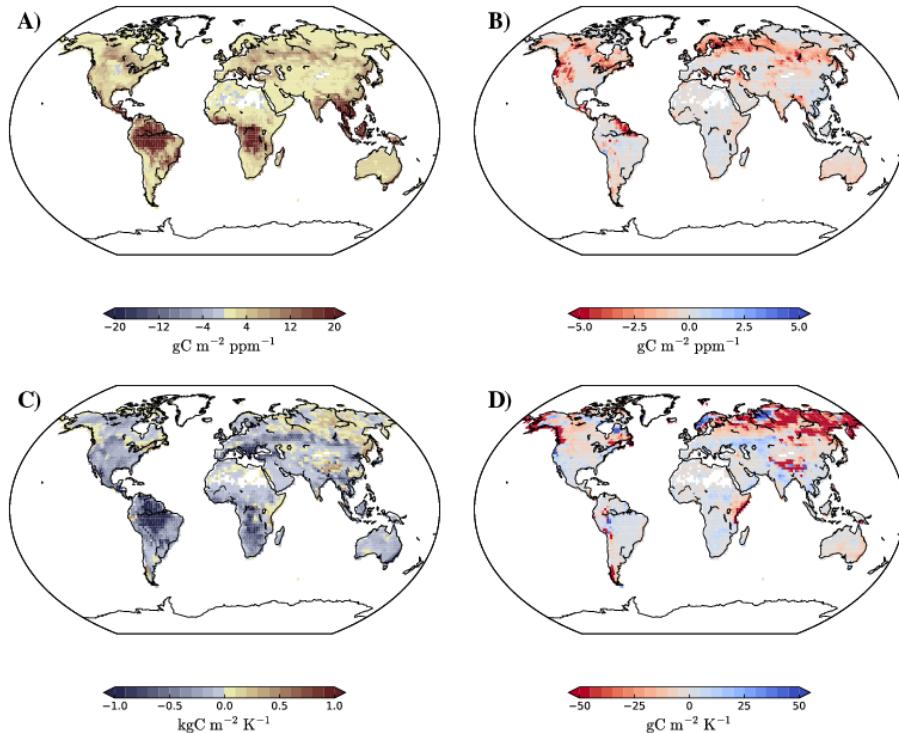
Figure 5. Spatial map of the carbon concentration feedback β_L (a) and the carbon climate feedback γ_L (c) (of the simulations with carbon-nitrogen interactions) as well as the effect of the nitrogen cycling on the respective feedbacks (b,d) (as the difference in the feedback strengths between simulations with and without carbon-nitrogen interactions).

Table 7. Carbon cycle feedbacks in simulations with JSBACH compared to results from CMIP5.

	Land carbon-concentration feedback $[Pg\,ppm^{-1}]$	Land carbon-climate feedback $[Pg\,^{\circ}C^{-1}]$	reference
CMIP5 MPI-ESM-LR	1.46	-83.2	Arora et al. (2013)
CMIP5 multi model mean	0.92±0.44	-58.5±28.5	Arora et al. (2013)
JSBACH C	0.74	-26.2	this study
JSBACH CN	0.61	-27.5	this study

effect of nitrogen availability on carbon storage is rather moderate in all simulation (Figure 2) due to the adjustments of the nitrogen balance to changes in the carbon cycle (Figure 4).

3.4 The effect of nitrogen on the carbon feedbacks

We quantify the strengths of the climate carbon-feedback (γ_L) and the carbon-concentration feedback (β_L) from the radiatively "coupled" and biogeochemically "coupled" simulations, respectively (Figure 5a,c). Both land feedbacks, with a global β_L of 0.61 Pg ppm^{-1} and a global γ_L of -27.5 Pg $^\circ C^{-1}$, are 34% and 53% smaller than the multi-model averages of the CMIP5

5 models, despite that the CMIP5 version of JSBACH simulated global β_L and γ_L which are 59% and 42% times larger than the average of CMIP5 models (Table 7).

In CMIP5 the two ESMs with nitrogen limitation (which shared the same terrestrial biosphere component) had feedback strengths 70–75% lower than averaged across models (Arora et al., 2013), suggesting a prominent role of nitrogen in dampening both carbon cycle feedbacks. Here, we find that the dampened response is primarily related to the modifications of the soil and

10 litter carbon decomposition module, rather than to the inclusion of the nitrogen cycle. The global β_L in the simulation without nitrogen cycle is only 10% larger than in the simulation with nitrogen, while there is hardly any difference in global γ_L between simulation, as the small positive and negative differences cancel out (Figure 5). This finding illustrates the need of a multitude of carbon-nitrogen models to draw conclusions regarding the effect of nitrogen on the land carbon feedbacks.

The large difference between the CMIP5 version of JSBACH and the recent version described here can primarily be attributed

15 to the new decomposition model. The drastically reduced γ_L is primarily caused by the smaller initial soil carbon stock, as well as by the long-term acclimation of decomposition to warming due to substrate depletion in YASSO (Goll et al., 2015). The importance of the initial soil carbon stock for the carbon losses due to warming was illustrated by Todd-Brown et al. (2014). The lower β_L can be attributed to a much lower fraction of biomass which is converted into stable soil organic matter. Therefore, the increasing productivity translates to a much smaller increase in carbon storage. JSBACH does not account for

20 the stimulation of decomposition of recalcitrant carbon under elevated CO_2 due to increases in labile organic matter (from of priming effect) observed in lab incubation experiments (Kuzyakov et al., 2000), which could potentially alter the response of soil carbon to increasing CO_2, but for which there is no evidence of its relevance on multi-decadal time scales (Cardinael et al., 2015).

A dampening effect of the nitrogen cycle on the response of the terrestrial carbon cycle to climate change and increasing CO_2

25 is in line with the majority of carbon-nitrogen model studies (Ciais et al., 2013; Zaehle, 2013), but not all (Esser et al., 2011; Warlind et al., 2014). The mechanism by which nitrogen can dampen β_L is via an increasing decoupling of gross primary productivity from biomass accumulation under increasing CO_2 concentration as mineral nitrogen availability decreases. In this case, the lack of nitrogen reduces the accumulation of carbon in vegetation biomass and respiration losses increase. The dampening of γ_L is mainly via an enhanced nitrogen mineralisation in cold regions due to warming (Zaehle, 2013; Warlind

30 et al., 2014; Koven et al., 2015), which cannot be fully captured by JSBACH due to assumption of CO_2-induced nutrient limitation, and therefore the model is prone to underestimate the effect of nitrogen on γ_L.

3.5 Model limitations and future development directions

The current understanding of processes governing the terrestrial nitrogen balance is still rather limited (Zaehle, 2013), and several processes which might be of importance, in particular stand dynamics (Warlind et al., 2014) which can potentially alter biomass turnover (Brienen et al., 2015), interactions between plants and microbes which can stimulate nitrogen scarcity by
5   non-altruistic symbioses (Franklin et al., 2014), and the availability of other nutrients (Goll et al., 2012) are not represented in JSBACH. In addition, the loss of organic matter in general due to erosion, although potentially of importance (Lal (2002) Lal, R.), is not yet represented in global land surface models, but development are underway (Naipal et al., 2015, 2016).

Regarding the processes resolved in JSBACH, the extent of BNF increase has to be regarded as highly uncertain, despite its agreement with short-term experiments (Liang et al., 2016): the formulation of BNF used here is based on an empirical
10   correlation between evapotranspiration and BNF and therefore the rate at which BNF rates increase strictly follows the increase in productivity whereas in reality the different processes leading to changes in BNF on ecosystem scales operate on a different time scale: The control of plants on their symbiotic partners via glucose export, and in case of nodules via oxygen regulation, result in changes in BNF from hours to months. On longer time scales, the composition of the ecosystem, namely the fraction of BNF associated species, affects nitrogen inputs to the system. While for tropical ecosystems there is evidence that any
15   governing mechanism(s) ought to operate at a synoptic scale (Hedin et al., 2009), higher latitude system might experience longer lag times. Additionally, other nutrients, like phosphorus or molybdenum, might slow down or reduce the potential of BNF to increase (Vitousek et al., 2013). Next generation BNF models, need to better resolve the governing mechanisms to increase the reliability of the simulated pace of changes in BNF.

Models which simulate simultaneous competition for soil nitrogen substrates by multiple processes match the observed
20   patterns of nitrogen losses better than models like JSBACH which are based on sequential competition (Niu et al., 2016). Here we find that despite the sequential competition, the simulated behavior is in general agreement with the dynamics of substrate-based mechanisms derived from manipulation experiments (Niu et al., 2016) and the spatial variability in the respective loss pathways is to a large degree in line with δ^{15}N-derived patterns.

The high-latitude permafrost processes are not represented here but were shown to be of importance for the effect on warming
25   on carbon and nitrogen losses. Permafrost regions store about 1,000 Gt C within the upper few meters of soil (Hugelius et al., 2014). The thawing of permafrost and deepening of the active layer in response to global warming can potentially lead to a much stronger climate carbon feedback (Schneider Von Deimling et al., 2012; Schuur et al., 2015). The recent study of Koven et al. (2015) with the CLM model showed these carbon losses in high latitudes can be partly offset by increased nitrogen mineralisation, and in turn productivity and input to the soils.

30   Finally, as advocated by for example Prentice et al. (2014); Medlyn et al. (2015), the stringent use of observational data set to evaluate the present day state of ecosystems as well as their response to manipulations must drive and guide new model developments whenever possible. With respect to JSBACH and other land surface models, the use of observation-derived climatology instead of the ESM climate as well as the use of site-specific simulations to allow a straightforward comparison to manipulation experiments is a research priority to increase the model reliability (Luo et al., 2012). In this study, the use of the

ESM climatology is justified by a focus on the feedback analysis in the framework of idealized simulations as suggested in the climate-carbon cycle model intercomparison project C4MIP (Anav et al., 2013; Jones et al., 2016). For further evaluation of the nitrogen limitation, however the preferable setup includes site-level simulations driven by observation-derived climatology (Zaehle et al., 2014).

4 Conclusions

The simulated response of primary productivity and the simulated variability in nitrogen loss pathways are in rather good agreement with observation based estimates despite the use of the simulated climate from an earth system model which in some regions deviates significantly from the observed climate (Hagemann et al., 2013). Regions with substantial bias in nitrogen loss pathways resemble regions with strong biases in either precipitation or surface temperature (Hagemann et al., 2013). The use of simulated climatology hampers a more detailed analysis of the nitrogen loss pathways and limits hampers the ability to evaluate land processes using observational based constraint. A more stringent use of observed climatology in the calibration of JSBACH is recommended due to increasingly more common application of JSBACH outside the earth system model as well as the increasing availability of observational constraints.

The effect of nitrogen cycling on the land carbon uptake in idealized simulations with JSBACH is globally minor, but not negligible. In particular, the carbon-concentration feedback is affected by mineral nitrogen availability, but the extent is moderate compared to earlier studies (Arora et al., 2013; Zaehle, 2013). During the first decades of the simulations, nitrogen limitation is circumpassed by a strong initial decline in loss terms in combination with increases in biological nitrogen fixation. Afterwards progressive increases in biological nitrogen fixation drive the accumulation of nitrogen in ecosystems. On top of that, warming enhances mineralisation and counteracts the immobilization of nitrogen in biomass. Our study is in line with the majority of carbon dioxide enrichment studies (Liang et al., 2016), showing that progressive nitrogen limitation under elevated carbon dioxide concentrations is less likely to occur than originally suggested (Luo et al., 2004).

The timescale and the extent to which the nitrogen cycle adjusts to increasing carbon dioxide and changing climate depend on the response of the input and loss processes of nitrogen as well as turnover of organic nitrogen. Here, we illustrate that the processes counteracting nitrogen scarcity operate on different time scales and have different trajectories due to differences in the respective environmental drivers, which indicates a picture more complicated than drawn from environmental response functions (Niu et al., 2016; Liang et al., 2016). It is difficult to assess to what extent the timescales in our experiments are realistic, as timescale on which these processes operate is well beyond the typical duration of manipulation experiments.

Our results suggest that nitrogen limitation of land carbon uptake of natural ecosystems could be temporally restricted, being the result of the inertia of the balancing processes (Altabet et al., 1995; Hedin et al., 2009). Ultimately, other nutrients like phosphorus which sources are depleted over time, are likely to dominate the long-term capacity of carbon storage.

5 Code availability

The JSBACH model version 3.10 used here includes the soil module YASSO and nitrogen components. The model version corresponds to the revision 8691 from the 19th July 2016 in the Apache version control system (SVN) of the Max Planck Institute for Meteorology (https://svn.zmaw.de/svn/cosmos/branches/mpiesm-landveg). This version will be used in the CMIP6 simulations, where other components (landuse, dynamic vegetation, fire) will be included as well. The source code of the CMIP6 version of JSBACH as a part of MPI-ESM will be available in 2017 under the MPI-M Software License Agreement obtained at http://www.mpimet.mpg.de/en/science/models/license/. In meantime, please contact Thomas Raddatz (thomas.raddatz@mpimet.mpg.de) for the code of the JSBACH if you plan an application of the model and envisage longer-term scientific collaboration.

6 Data availability

Primary data and scripts used in the analysis and other supplementary information that may be useful in reproducing the author's work are archived by the Max Planck Institute for Meteorology and can be obtained by contacting publications@mpimet.mpg.de.

Author contributions. The study was led by Daniel S. Goll who developed the model concept and implemented it into JSBACH. Victor Brovkin, Alexander J. Winkler and Thomas Raddatz designed and performed the model experiment. Alexander J. Winkler analysed and visualized the data. Ning Dong and Colin Prentice performed the estimation of the nitrogen loss pathways. Philippe Ciais contributed to the analysis and evaluation of the model. The draft of the manuscript was written by Daniel S. Goll with all authors contributing to its final form.

Competing interests. The authors declare that they have no conflict of interest.

Acknowledgements. This work was initiated when Daniel Goll was funded through the DFG Cluster of Excellence CLiSAP (EXC 177/2), now he is funded by the "IMBALANCE-P" project of the European Research Council (ERC-2013-SyG-610028). This work contributes to the H2020 project CRESCENDO, which receives funding from the European Union's Horizon 2020 research and innovation programme under grant agreement no. 641816. DN was supported by an international Macquarie University Research Scholarship and by the Ecosystem Modelling and Scaling Infrastructure (eMAST, http://www.emast.org.au) facility of the Terrestrial Ecosystem Research Network. This work is a contribution to the AXA Chair Programme in Biosphere and Climate Impacts and the Imperial College initiative on Grand Challenges in Ecosystems and the Environment (ICP). We thank Christian Reick and Daniela Kracher for discussing the nitrogen model implementation, and Christian Wirth and Hans Cornelissen for discussions of woody litter decomposition. We thank Thomas Kleinen for reviewing the manuscript prior submission. We acknowledge the World Climate Research Programme's Working Group on Coupled Modelling, which is responsible for CMIP, and we thank the climate modeling group at the Max Planck Insitute for Meteorology producing and making available their model output. For CMIP the U.S. Department of Energy's Program for Climate Model Diagnosis and Intercomparson provides coordinating support and led development of software infrastructure in partnership with the Global Organization for Earth System Science Portals.

References

Altabet, M. a., Francois, R., Murray, D. W., and Prell, W. L.: Climate-related variations in denitrification in the Arabian Sea from sediment 15N/14N ratios, Nature, 373, 506–509, doi:10.1038/373506a0, 1995.

Anav, A., Friedlingstein, P., Kidston, M., Bopp, L., Ciais, P., Cox, P., Jones, C., Jung, M., Myneni, R., and Zhu, Z.: Evaluating the Land and Ocean Components of the Global Carbon Cycle in the Cmip5 Earth System Models, J. Clim., p. 130401082723008, doi:10.1175/JCLI-D-12-00417.1, http://journals.ametsoc.org/doi/abs/10.1175/JCLI-D-12-00417.1, 2013.

Arora, V. K., Boer, G. J., Friedlingstein, P., Eby, M., Jones, C. D., Christian, J. R., Bonan, G., Bopp, L., Brovkin, V., Cadule, P., Hajima, T., Ilyina, T., Lindsay, K., Tjiputra, J. F., and Wu, T.: Carbon-concentration and carbon-climate feedbacks in CMIP5 Earth system models, Journal of Climate, p. 130208091306008, doi:10.1175/JCLI-D-12-00494.1, http://journals.ametsoc.org/doi/abs/10.1175/JCLI-D-12-00494.1, 2013.

Bai, E., Houlton, B. Z., and Wang, Y. P.: Isotopic identification of nitrogen hotspots across natural terrestrial ecosystems, Biogeosciences, 9, 3287–3304, doi:10.5194/bg-9-3287-2012, 2012.

Brienen, R. J. W., Phillips, O. L., Feldpausch, T. R., and Et Al.: Long-term decline of the Amazon carbon sink, Nature, 519, 344–348, doi:10.1038/nature14283, http://dx.doi.org/10.1038/nature14283, 2015.

Campbell, G. S. and Norman, J. M.: An Introduction to Environmental Biophysic, Springer-Verlag New York, 2 edn., doi:10.1007/978-1-4612-1626-1.

Canion, A., Kostka, J. E., Gihring, T. M., Huettel, M., Van Beusekom, J. E. E., Gao, H., Lavik, G., and Kuypers, M. M. M.: Temperature response of denitrification and anammox reveals the adaptation of microbial communities to in situ temperatures in permeable marine sediments that span 50 in latitude, Biogeosciences, 11, 309–320, doi:10.5194/bg-11-309-2014, 2014.

Cardinael, R., Eglin, T., Guenet, B., Neill, C., Houot, S., and Chenu, C.: Is priming effect a significant process for long-term SOC dynamics? Analysis of a 52-years old experiment, Biogeochemistry, 123, 203–219, doi:10.1007/s10533-014-0063-2, http://dx.doi.org/10.1007/s10533-014-0063-2, 2015.

Cheng, W., Chen, Q., Xu, Y., Han, X., and Li, L.: Climate and ecosystem15N natural abundance along a transect of Inner Mongolian grasslands: Contrasting regional patterns and global patterns, Global Biogeochemical Cycles, 23, 1–11, doi:10.1029/2008GB003315, 2009.

Ciais, P., Sabine, C., Bala, G., Bopp, L., Brovkin, V., Canadell, J., Chhabra, a., DeFries, R., Galloway, J., Heimann, M., Jones, C., Quéré, C. L., Myneni, R., Piao, S., Thornton, P., France, P. C., Willem, J., Friedlingstein, P., and Munhoven, G.: 2013: Carbon and Other Biogeochemical Cycles, in: Climate Change 2013: The Physical Science Basis. Contribution of Working Group I to the Fifth Assessment Report of the Intergovernmental Panel on Climate Change., edited by Stocker, T., Qin, D., Plattner, G.-K., Tignor, M., Allen, S. K., Boschug, J., Nauels, A., Y., X., Bex, V., and Midgley, P. M., chap. Carbon and, pp. 465–570, Cambridge University Press, Cambridge, United Kingdom and New York, NY, USA, doi:10.1017/CBO9781107415324.015, 2013.

Cleveland, C. C., Townsend, A. R., Schimel, D. S., Fisher, H., Hedin, L. O., Perakis, S., Latty, E. F., Fischer, C. V., Elseroad, A., and Wasson, M. F.: Global patterns of terrestrial biological nitrogen (N2) fixation in natural ecosystems, Global Biochemical Cycles, 13, 623–645, doi:10.1029/1999GB900014, http://onlinelibrary.wiley.com/doi/10.1029/1999GB900014/pdf, 1999.

Ehlers, I., Augusti, A., Betson, T. R., Nilsson, M. B., Marshall, J. D., and Schleucher, J.: Detecting long-term metabolic shifts using isotopomers : CO 2 -driven suppression of photorespiration in C 3 plants over the 20th century, Proceedings of the National Academy of Sciences, pp. 1–6, doi:10.1073/pnas.1504493112, 2015.

Esser, G., Kattge, J., Sakalli, A., and Use, L.: Feedback of carbon and nitrogen cycles enhances carbon sequestration in the terrestrial biosphere, GLOBAL CHANGE BIOLOGY, 17, 819–842, doi:10.1111/j.1365-2486.2010.02261.x, 2011.

Eyring, V., Bony, S., Meehl, J., Senior, C., Stouffer, R., Taylor, K., and Panel, C.: Overview of the Coupled Model Intercomparison Project Phase 6 (CMIP6) Experimental Design and Organization Coupled Model Intercomparison Project (CMIP), 6, doi:10.5194/gmd-9-1937-2016, 2016.

Fang, Y., Yoh, M., Koba, K., Zhu, W., Takebayashi, Y., Xiao, Y., Lei, C., Mo, J., Zhang, W., and Lu, X.: Nitrogen deposition and forest nitrogen cycling along an urban-rural transect in southern China, Global Change Biology, 17, 872–885, doi:10.1111/j.1365-2486.2010.02283.x, 2011.

Fang, Y., Koba, K., Yoh, M., Makabe, A., and Liu, X.: Patterns of foliar 15N and their control in Eastern Asian forests, Ecological Research, 28, 735–748, doi:10.1007/s11284-012-0934-8, http://dx.doi.org/10.1007/s11284-012-0934-8, 2013.

Franklin, O., Näsholm, T., Högberg, P., and Högberg, M. N.: Forests trapped in nitrogen limitation - an ecological market perspective on ectomycorrhizal symbiosis, New Phytologist, 203, 657–666, doi:10.1111/nph.12840, http://www.ncbi.nlm.nih.gov/pubmed/24824576, 2014.

Friedlingstein, P., Cox, P., Betts, R., Bopp, L., Von Bloh, W., Brovkin, V., Cadule, P., Doney, S., Eby, M., Fung, I., Bala, G., John, J., Jones, C., Joos, F., Kato, T., Kawamiya, M., Knorr, W., Lindsay, K., Matthews, H. D., Raddatz, T., Rayner, P., Reick, C., Roeckner, E., Schnitzler, K. G., Schnur, R., Strassmann, K., Weaver, A. J., Yoshikawa, C., and Zeng, N.: Climate-carbon cycle feedback analysis: Results from the (CMIP)-M-4 model intercomparison, JOURNAL OF CLIMATE, 19, 3337–3353, 2006.

Galloway, J. N., Dentener, F. J., Capone, D. G., Boyer, E. W., Howarth, R. W., Seitzinger, S. P., Asner, G. P., Cleveland, C. C., Green, P. a., Holland, E. A., Karl, D. M., Michaels, A. F., Porter, J. H., Townsend, a. R., and Vo, C. J.: Nitrogen cycles : past, present , and future, BIOGEOCHEMISTRY, 70, 153–226, 2004.

Galloway, J. N., Leach, A. M., Bleeker, A., and Erisman, J. W.: A chronology of human understanding of the nitrogen cycle., Philosophical transactions of the Royal Society of London. Series B, Biological sciences, 368, 20130 120, doi:10.1098/rstb.2013.0120, http://www.pubmedcentral.nih.gov/articlerender.fcgi?artid=3682740{&}tool=pmcentrez{&}rendertype=abstract, 2013.

Goll, D. S., Brovkin, V., Parida, B. R., Reick, C. H., Kattge, J., Reich, P. B., Van Bodegom, P. M., and Niinemets, Ü.: Nutrient limitation reduces land carbon uptake in simulations with a model of combined carbon, nitrogen and phosphorus cycling, Biogeosciences, 9, 3547–3569, doi:10.5194/bg-9-3547-2012, http://www.biogeosciences-discuss.net/9/3173/2012/http://www.biogeosciences.net/9/3547/2012/, 2012.

Goll, D. S., Brovkin, V., Liski, J., Raddatz, T., Thum, T., and Todd-Brown, K. E. O.: Strong dependence of CO2 emissions from anthropogenic land cover change on soil carbon parametrization and initial land cover, Global Biogeochemical Cycles, 29, 1–58, doi:10.1002/2014GB004988.Abstract, 2015.

Hagemann, S. and Stacke, T.: Impact of the soil hydrology scheme on simulated soil moisture memory, Climate Dynamics, pp. 1731–1750, doi:10.1007/s00382-014-2221-6, 2014.

Hagemann, S., Loew, A., and Andersson, A.: Combined evaluation of MPI-ESM land surface water and energy fluxes, J. Adv. Model. Earth Syst., 5, n/a–n/a, doi:10.1029/2012MS000173, http://doi.wiley.com/10.1029/2012MS000173, 2013.

Hedin, L. O., Armesto, J. J., and Johnson, R. A. H.: Patterns of Nutrient Loss from Unpolluted, Old-Growth Temperate Forests: Evaluation of Biogeochemical Theory, ECOLOGY, 76, 493–509, doi:10.2307/1941208, 1995.

Hedin, L. O., Brookshire, E. J., Menge, D. N., and Barron, A. R.: The Nitrogen Paradox in Tropical Forest Ecosystems, Annual Review of Ecology, Evolution, and Systematics, 40, 613–635, doi:10.1146/annurev.ecolsys.37.091305.110246, http://www.annualreviews.org/doi/abs/10.1146/annurev.ecolsys.37.091305.110246, 2009.

Hilton, R. G., Galy, A., West, A. J., Hovius, N., and Roberts, G. G.: Geomorphic control on the ??15N of mountain forests, Biogeosciences, 5   10, 1693–1705, doi:10.5194/bg-10-1693-2013, 2013.

Houlton, B. Z. and Bai, E.: Imprint of denitrifying bacteria on the global terrestrial biosphere, Proc. Natl. Acad. Sci. USA, 106, 21 713–21 716, doi:10.1073/pnas.0912111106, 2009.

Houlton, B. Z., Marklein, A. R., and Bai, E.: Representation of nitrogen in climate change forecasts, Nature Climate Change, 5, 398–401, doi:10.1038/nclimate2538, http://www.nature.com/doifinder/10.1038/nclimate2538, 2015.

10   Hugelius, G., Strauss, J., Zubrzycki, S., Harden, J. W., Schuur, E. A. G., Ping, C. L., Schirrmeister, L., Grosse, G., Michaelson, G. J., Koven, C. D., O'Donnell, J. A., Elberling, B., Mishra, U., Camill, P., Yu, Z., Palmtag, J., and Kuhry, P.: Estimated stocks of circumpolar permafrost carbon with quantified uncertainty ranges and identified data gaps, Biogeosciences, 11, 6573–6593, doi:10.5194/bg-11-6573-2014, 2014.

Hungate, B. a., Dukes, J. S., Shaw, M. R., Luo, Y., and Field, C. B.: Nitrogen and Climate Change, Science, 302, 1512–1513, doi:10.1126/science.1091390, http://www.sciencemag.org/content/302/5650/1512.short, 2003.

15   Hurtt, G. C.,Chini, L. P.,Frolking, S.,Betts, R. a.,Feddema, J.,Fischer, G.,Fisk, J. P. ,Hibbard, K.,Houghton, R. a.Janetos, A.,Jones, C. D.,Kindermann, G. ,Kinoshita, T.,Klein Goldewijk, Kees,Riahi, K.,Shevliakova, E., Smith, S.,Stehfest, E.,Thomson, A.,Thornton, P.,Vuuren, D. P., and Wang, Y. P : Harmonization of land-use scenarios for the period 1500–2100: 600 years of global gridded annual land-use transitions, wood harvest, and resulting secondary lands, Clim. Change, 109, 117–161, doi:10.1007/s10584-011-0153-2, 2011.

Ito, A.: A historical meta-analysis of global terrestrial net primary productivity: are estimates converging?, Global Change Biology, 17, 20   3161–3175, doi:10.1111/j.1365-2486.2011.02450.x, http://doi.wiley.com/10.1111/j.1365-2486.2011.02450.x, 2011.

Jones, C. D., Arora, V., Friedlingstein, P., Bopp, L., Brovkin, V., Dunne, J., Graven, H., Hoffman, F., Ilyina, T., John, J. G., Jung, M., Kawamiya, M., Koven, C., Pongratz, J., Raddatz, T., Randerson, J., and Zaehle, S.: The C4MIP experimental protocol for CMIP6, Geoscientific Model Development Discussions, pp. 1–52, doi:10.5194/gmd-2016-36, http://www.geosci-model-dev-discuss.net/gmd-2016-36/, 2016.

25   Koven, C. D., Lawrence, D. M., and Riley, W. J.: Permafrost carbon-climate feedback is sensitive to deep soil carbon decomposability but not deep soil nitrogen dynamics., Proceedings of the National Academy of Sciences of the United States of America, 112, 3752–7, doi:10.1073/pnas.1415123112, http://www.pnas.org/content/112/12/3752.full, 2015.

Kuzyakov, Y., Friedel, J. K., and Stahr, K.: Review of mechanisms and quantification of priming effects, Soil Biology and Biochemistry, 32, 1485–1498, doi:10.1016/S0038-0717(00)00084-5, 2000.

30   Lal, R.: Soil erosion and the global carbon budget, Environment International , 29, 437–450, doi:10.1016/S0160-4120(02)00192-7, 2002.

Liang, J., Qi, X., Souza, L., and Luo, Y.: Processes regulating progressive nitrogen limitation under elevated carbon dioxide: A meta-analysis, Biogeosciences, 13, 2689–2699, doi:10.5194/bg-13-2689-2016, 2016.

Luo, Y., Su, B., Currie, W. S., Dukes, J. S., Finzi, A. C., Hartwig, U., Hungate, B., McMurtrie, R. E., Oren, R., Parton, W. J., Pataki, D. E., Shaw, M. R., Zak, D. R., and Field, C. B.: Progressive Nitrogen Limitation of Ecosystem Responses to Rising Atmospheric Carbon 35   Dioxide, BIOSCIENCE, 54, 731–739, doi:10.1641/0006-3568(2004)054[0731:PNLOER]2.0.CO;2, 2004.

McCarthy, H. R. and Pataki, D. E.: Drivers of variability in water use of native and non-native urban trees in the greater Los Angeles area, Urban Ecosystems, 13, 393–414, doi:10.1007/s11252-010-0127-6, 2010.

Medlyn, B. E., Kauwe, M. G. D., Walker, A. P., Dietze, C., Hanson, P., Hickler, T., Jain, A., Luo, Y., Parton, W., Colin, I., Wang, S., Wang, Y.-p., Weng, E., Iversen, C. M., Mccarthy, H., Warren, J., Oren, R., Norby, R., Division, E. S., Ridge, O., Goethe, G., and Collins, F.: Using Ecosystem Experiments to Improve Vegetation Models : Lessons Learnt from the Free-Air CO 2 Enrichment Model-Data Synthesis, Nature Climate Change, 5, 528–534, doi:10.1038/nclimate2621, 2015.

Meixner, T. and Bales, R. C.: Hydrochemical modeling of coupled C and N cycling in high-elevation catchments: importance of snow cover, Biogeochemistry, 62, 289–308, doi:10.1023/A:1021118922787, 2002.

Naipal, V., Reick, C., Pongratz, J., and Oost, K. V.: Improving the global applicability of the RUSLE model – adjustment of the topographical and rainfall erosivity factors, Geosci. Model Dev., 8, 2893–2913, doi:10.5194/gmd-8-2893-2015, 2015.

Naipal, V., Reick, C., Van Oost, K., Hoffmann, T., and Pongratz, J.: Modeling long-term, large-scale sediment storage using a simple sediment budget approach, Earth Surface Dynamics, 4, 407–423, doi:10.5194/esurf-4-407-2016, 2016.

New, M., Lister, D., Hulme, M., and Makin, I.: A high-resolution data set of surface climate over global land areas, Climate Research, 21, 1–25, doi:10.3354/cr021001, 2002.

Niu, S., Classen, A. T., Dukes, J. S., Kardol, P., Liu, L., Luo, Y., Rustad, L., Sun, J., Tang, J., Templer, P. H., Thomas, R. Q., Tian, D., Vicca, S., Wang, Y. P., Xia, J., and Zaehle, S.: Global patterns and substrate-based mechanisms of the terrestrial nitrogen cycle, Ecology Letters, 19, 697–709, doi:10.1111/ele.12591, 2016.

Norby, R. J., DeLucia, E. H., Gielen, B., Calfapietra, C., Giardina, C. P., King, J. S., Ledford, J., McCarthy, H. R., Moore, D. J. P., Ceulemans, R., De Angelis, P., Finzi, A. C., Karnosky, D. F., Kubiske, M. E., Lukac, M., Pregitzer, K. S., Scarascia-Mugnozza, G. E., Schlesinger, W. H., and Oren, R.: Forest response to elevated CO2 is conserved across a broad range of productivity, Proceedings of the National Academy of Sciences, 102, 18 052–18 056, doi:10.1073/pnas.0509478102, http://www.pnas.org/cgi/doi/10.1073/pnas.0509478102{%}5Cnhttp://www.pnas.org/content/102/50/18052.full{%}5Cnhttp://www.pnas.org/cgi/doi/10.1073/pnas.0509478102, 2005.

Norby, R. J., Warren, J. M., Iversen, C. M., Medlyn, B. E., and McMurtrie, R. E.: CO2 enhancement of forest productivity constrained by limited nitrogen availability., Proceedings of the National Academy of Sciences of the United States of America, 107, 19 368–19 373, doi:10.1073/pnas.1006463107, 2010.

Norby, R. J., De Kauwe, M. G., Domingues, T. F., Duursma, R. A., Ellsworth, D. S., Goll, D. S., Lapola, D. M., Luus, K. A., MacKenzie, A. R., Medlyn, B. E., Pavlick, R., Rammig, A., Smith, B., Thomas, R., Thonicke, K., Walker, A. P., Yang, X., and Zaehle, S.: Model-data synthesis for the next generation of forest free-air CO2 enrichment (FACE) experiments., The New phytologist, doi:10.1111/nph.13593, http://www.ncbi.nlm.nih.gov/pubmed/26249015, 2015.

Parida, B. R.: The influence of plant nitrogen availability on the global carbon cycle and N O emissions, in: Berichte zur Erdsystemforschung, 2011.

Parton, W. J., Scurlock, J. M. O., Ojima, D. S., Gilmanov, T. G., Scholes, R. J., Schimel, D. S., Kirchner, T., Menaut, J.-C., Seastedt, T. R., Garcia Moya, E., Kamnalrut, A., and Kinyamario, J. I.: Observations and modeling of biomass and soil organic matter dynamics for the grassland biome worldwide, Global Biogeochemical Cycles, 7, 785–809, doi:10.1029/93GB02042, 1993.

Patino, S., Lloyd, J., Paiva, R., Baker, T. R., Quesada, C. A., Mercado, L. M., Schmerler, J., Schwarz, M., Santos, A. J. B., Aguilar, A., Czimczik, C. I., Gallo, J., Horna, V., Hoyos, E. J., Jimenez, E. M., Palomino, W., Peacock, J., Pena-Cruz, A., Sarmiento, C., Sota, A., Turriago, J. D., Villanueva, B., Vitzthum, P., Alvarez, E., Arroyo, L., Baraloto, C., Bonal, D., Chave, J., Costa, A. C. L., Herrera, R., Higuchi, N., Killeen, T., Leal, E., Luizao, F., Meir, P., Monteagudo, A., Neil, D., Nunez-Vargas, P., Penuela, M. C., Pitman, N., Priante Filho, N., Prieto, A., Panfil, S. N., Rudas, A., Salomao, R., Silva, N., Silveira, M., DeAlmeida, S. S., Torres-Lezama, A., Vasquez-Martinez,

R., Vieira, I., Malhi, Y., and Phillips, O. L.: Branch xylem density variations across the Amazon Basin, BIOGEOSCIENCES, 6, 545–568, 2009.

Peri, P. L., Ladd, B., Pepper, D. A., Bonser, S. P., Laffan, S. W., and Amelung, W.: Carbon (?? 13C) and nitrogen (?? 15N) stable isotope composition in plant and soil in Southern Patagonia's native forests, Global Change Biology, 18, 311–321, doi:10.1111/j.1365-2486.2011.02494.x, 2012.

Prentice, I. C., Liang, X., Medlyn, B. E., and Wang, Y.-P.: Reliable, robust and realistic: the three R's of next-generation land surface modelling, Atmospheric Chemistry and Physics Discussions, 14, 24 811–24 861, doi:10.5194/acpd-14-24811-2014, http://www.atmos-chem-phys-discuss.net/14/24811/2014/, 2014.

, Pongratz, J., C. Reick, T. Raddatz, and M. Claussen: A reconstruction of global agricultural areas and land cover for the last millennium, Global Biogeochem. Cycles, 22, doi:10.1029/2007GB003153, 2008.

Raddatz, T. J., Reick, C. H., Knorr, W., Kattge, J., Roeckner, E., Schnur, R., Schnitzler, K.-G. G., Wetzel, P., and Jungclaus, J.: Will the tropical land biosphere dominate the climate-carbon cycle feedback during the twenty-first century?, CLIMATE DYNAMICS, 29, 565–574, doi:10.1007/s00382-007-0247-8, 2007.

Rütting, T.: Nitrogen mineralization, not N$_2$ fixation alleviates progressive nitrogen limitation – Comment on "Processes regulating progressive nitrogen limitation under elevated carbon dioxide: a meta-analysis" b, Biogeosciences Discussions, pp. 1–8, doi:10.5194/bg-2016-456, http://www.biogeosciences-discuss.net/bg-2016-456/, 2016.

Schneider Von Deimling, T., Meinshausen, M., Levermann, A., Huber, V., Frieler, K., Lawrence, D. M., and Brovkin, V.: Estimating the near-surface permafrost-carbon feedback on global warming, Biogeosciences, 9, 649–665, doi:10.5194/bg-9-649-2012, 2012.

Schuur, E. a. G., McGuire, a. D., Schädel, C., Grosse, G., Harden, J. W., Hayes, D. J., Hugelius, G., Koven, C. D., Kuhry, P., Lawrence, D. M., Natali, S. M., Olefeldt, D., Romanovsky, V. E., Schaefer, K., Turetsky, M. R., Treat, C. C., and Vonk, J. E.: Climate change and the permafrost carbon feedback, Nature, 520, 171–179, doi:10.1038/nature14338, http://www.nature.com/doifinder/10.1038/nature14338, 2015.

Shi, Z., Sherry, R., Xu, X., Hararuk, O., Souza, L., Jiang, L., Xia, J., Liang, J., and Luo, Y.: Evidence for long-term shift in plant community composition under decadal experimental warming, Journal of Ecology, 103, 1131–1140, doi:10.1111/1365-2745.12449, 2015.

Sommer, J., Pausch, J., Brundrett, M. C., Dixon, K. W., Bidartondo, M. I., and Gebauer, G.: Limited carbon and mineral nutrient gain from mycorrhizal fungi by adult Australian Orchids, American Journal of Botany, 99, 1133–1145, doi:10.3732/ajb.1100575, 2012.

Sullivan, B. W., Smith, W. K., Townsend, A. R., Nasto, M. K., Reed, S. C., Chazdon, R. L., and Cleveland, C. C.: Spatially robust estimates of biological nitrogen (N) fixation imply substantial human alteration of the tropical N cycle., Proceedings of the National Academy of Sciences of the United States of America, 111, 8101–6, doi:10.1073/pnas.1320646111, http://www.ncbi.nlm.nih.gov/pubmed/24843146, 2014.

Taylor, K. E.: Summarizing multiple aspects of model performance in a single diagram, Journal of Geophysical Research, 106, 7183–7192, 2001.

Taylor, K. E., Stouffer, R. J., and Meehl, G. a.: An Overview of CMIP5 and the Experiment Design, Bull. Am. Meteorol. Soc., 93, 485–498, doi:10.1175/BAMS-D-11-00094.1, http://journals.ametsoc.org/doi/abs/10.1175/BAMS-D-11-00094.1, 2012.

Thomas, R. Q., Zaehle, S., Templer, P. H., and Goodale, C. L.: Global patterns of nitrogen limitation: Confronting two global biogeochemical models with observations, Global Change Biology, 19, 2986–2998, doi:10.1111/gcb.12281, 2013.

Thornton, P. E., Rosenbloom, N. a., Mahowald, N. M., Lamarque, J. F. J.-F., Rosenbloom, N. a., and Mahowald, N. M.: Influence of carbon-nitrogen cycle coupling on land model response to CO2 fertilization and climate variability, GLOBAL BIOGEOCHEMICAL CYCLES, 21, 1–15, doi:10.1029/2006GB002868, 2007.

Todd-Brown, K. E. O., Randerson, J. T., Post, W. M., Hoffman, F. M., Tarnocai, C., Schuur, E. a. G., and Allison, S. D.: Causes of variation in soil carbon simulations from CMIP5 Earth system models and comparison with observations, Biogeosciences, 10, 1717–1736, doi:10.5194/bg-10-1717-2013, http://www.biogeosciences.net/10/1717/2013/, 2013.

Todd-Brown, K. E. O., Randerson, J. T., Hopkins, F., Arora, V., Hajima, T., Jones, C., Shevliakova, E., Tjiputra, J., Volodin, E., Wu, T., Zhang, Q., and Allison, S. D.: Changes in soil organic carbon storage predicted by Earth system models during the 21st century, Biogeosciences, 11, 2341–2356, doi:10.5194/bg-11-2341-2014, http://www.biogeosciences.net/11/2341/2014/, 2014.

Tuomi, M., Vanhala, P., Karhu, K., Fritze, H., and Liski, J.: Heterotrophic soil respiration—Comparison of different models describing its temperature dependence, Ecological Modelling, 211, 182–190, doi:10.1016/j.ecolmodel.2007.09.003, http://linkinghub.elsevier.com/retrieve/pii/S030438000700453X, 2008.

Tuomi, M., Thum, T., Järvinen, H., Fronzek, S., Berg, B., Harmon, M., Trofymow, J., Sevanto, S., and Liski, J.: Leaf litter decomposition—Estimates of global variability based on Yasso07 model, Ecological Modelling, 220, 3362–3371, doi:10.1016/j.ecolmodel.2009.05.016, http://linkinghub.elsevier.com/retrieve/pii/S030438000900386X, 2009.

Tuomi, M., Laiho, R., Repo, A., and Liski, J.: Wood decomposition model for boreal forests, Ecological Modelling, 222, 709–718, doi:10.1016/j.ecolmodel.2010.10.025, http://linkinghub.elsevier.com/retrieve/pii/S0304380010005855, 2011.

Viani, R. A. G., Rodrigues, R. R., Dawson, T. E., and Oliveira, R. S.: Functional differences between woodland savannas and seasonally dry forests from south-eastern Brazil: Evidence from 15N natural abundance studies, Austral Ecology, 36, 974–982, doi:10.1111/j.1442-9993.2010.02233.x, 2011.

Vitousek, P. M., Menge, D. N. L., Reed, S. C., and Cleveland, C. C.: Biological nitrogen fixation: rates, patterns and ecological controls in terrestrial ecosystems., Philosophical transactions of the Royal Society of London. Series B, Biological sciences, 368, 20130119, doi:10.1098/rstb.2013.0119, http://www.ncbi.nlm.nih.gov/pubmed/23713117, 2013.

Wang, Y.-P. P., Law, R. M., and Pak, B.: A global model of carbon, nitrogen and phosphorus cycles for the terrestrial biosphere, Biogeosciences, 7, 2261–2282, doi:10.5194/bg-7-2261-2010, 2010.

Warlind, D., Smith, B., Hickler, T., and Arneth, A.: Nitrogen feedbacks increase future terrestrial ecosystem carbon uptake in an individual-based dynamic vegetation model, Biogeosciences, 11, 6131–6146, doi:10.5194/bg-11-6131-2014, 2014.

Weedon, G. P., Gomes, S., Viterbo, P., Shuttleworth, W. J., Blyth, E., Österle, H., Adam, J. C., Bellouin, N., Boucher, O., and Best, M.: Creation of the WATCH Forcing Data and Its Use to Assess Global and Regional Reference Crop Evaporation over Land during the Twentieth Century, Journal of Hydrometeorology, 12, 823–848, doi:10.1175/2011JHM1369.1, http://journals.ametsoc.org/doi/abs/10.1175/2011JHM1369.1, 2011.

Wieder, W. R., Cleveland, C. C., Smith, W. K., and Todd-Brown, K.: Future productivity and carbon storage limited by terrestrial nutrient availability, Nature Geoscience, 8, 1–15, doi:10.1038/ngeo2413, http://www.nature.com/doifinder/10.1038/ngeo2413, 2015.

Xu-Ri, Prentice, I. C., and Academy, C.: Terrestrial nitrogen cycle simulation with a dynamic global vegetation model, Global Change Biol., 14, 1745–1764, doi:10.1111/j.1365-2486.2008.01625.x, http://dx.doi.org/10.1111/j.1365-2486.2008.01625.x, 2008.

Yi, X. and Yang, Y.: Independence of alpine meadow plants from soil organic matter for nitrogen supply: evidence from stable nitrogen isotopes, Isotopes in environmental and health studies, 43, 51–56, 2007.

Zaehle, S.: Terrestrial nitrogen - carbon cycle interactions at the global scale, Philosophical transactions of the Royal Society of London. Series B, Biological sciences, 368, doi:http://dx.doi.org/10.1098/rstb.2013.0125, 2013.

Zaehle, S., Jones, C. D., Houlton, B., Lamarque, J.-F., and Robertson, E.: Nitrogen availability reduces CMIP5 projections of 21st century land carbon uptake, Journal of Climate, doi:10.1175/JCLI-D-13-00776.1, http://journals.ametsoc.org/doi/abs/10.1175/JCLI-D-13-00776.1, 2014.

Zaehle, Sönke, Medlyn, Belinda E, De Kauwe, Martin G, Walker, Anthony P, Dietze, Michael C, Hickler, Thomas, Luo, Yiqi, Wang, Ying-Ping, El-masri, Bassil, Thornton, Peter, Jain, Atul, Wang, Shusen, Warlind, David, Weng, Ensheng, Parton, William, Iversen, Colleen M, Gallet-budynek, Anne, Mccarthy, Heather, Finzi, Adrien C., Hanson, Paul J., Prentice, Iain Colin, Oren, Ram, and Norby, Richard J.: Evaluation of 11 terrestrial carbon-nitrogen cycle models against observations from two temperate Free-Air CO2 Enrichment studies, New Phytologist, doi:10.1111/nph.12697, 2014.

Zhang, L., Hickel, K., Dawes, W. R., Chiew, F. H. S., Western, A. W., and Briggs, P. R.: A rational function approach for estimating mean annual evapotranspiration, Water Resources Research, 40, 1–14, doi:10.1029/2003WR002710, 2004.